Effects of polarization-mode dispersion on fiber-based parametric amplification and wavelength conversion

Qiang Lin and Govind P. Agrawal

Institute of Optics, University of Rochester, Rochester, New York 14627

Received October 30, 2003

We present a vector theory of four-wave mixing in optical fibers and use it to discuss the effect of polarization-mode dispersion (PMD) on the performance of parametric amplifiers and wavelength converters. We show that PMD distorts the gain spectrum and makes it less uniform than that expected in the absence of residual birefringence. PMD also induces large fluctuations in the amplified or wavelength-converted signal.

OCIS codes: 060.4370, 190.4380, 260.5430.

Fiber-optic parametric amplifiers (FOPAs), based on four-wave mixing (FWM) occurring inside optical fibers, can provide high gain over a relatively wide bandwidth.[1–3] However, the underlying FWM process is highly polarization dependent.[4] Residual birefringence inside optical fibers not only randomizes the state of polarization (SOP) of any optical wave but also induces differential polarization variations among waves of different frequencies through polarization-mode dispersion (PMD).[5] In the presence of PMD the pump, signal, and idler waves cannot maintain their relative SOPs along the fiber, resulting in degradation of the FOPA performance unless a polarization-maintaining fiber is used. Moreover, since PMD can change with time because of environmental variations, it would induce fluctuations in the amplified signal in practice. Although PMD effects have been observed in experiments,[3,6–8] a theory describing such effects is not yet fully developed. In this Letter we present a vector theory for the degenerate FWM process and use it to show that the output of the FOPAs and wavelength converters is significantly affected by residual birefringence and can fluctuate over a wide range.

Using the general form of the nonlinear polarization for silica glass[4] and introducing the Jones vectors $|A_p\rangle$, $|A_s\rangle$, and $|A_i\rangle$ associated with the pump, signal, and idler waves, respectively, in the notation of Ref. 5, we obtain the following set of coupled vector equations governing the degenerate FWM process in an optical fiber pumped with a single intense wave as $2\omega_p = \omega_s + \omega_i$:

$$\frac{\mathrm{d}|A_p\rangle}{\mathrm{d}z} = i\left(\beta_p - \frac{1}{2}\omega_p \mathbf{B}\cdot\boldsymbol{\sigma}\right)|A_p\rangle + \frac{i\gamma}{3}\left(2\langle A_p|A_p\rangle + |A_p^*\rangle\langle A_p^*|\right)|A_p\rangle, \tag{1}$$

$$\frac{\mathrm{d}|A_s\rangle}{\mathrm{d}z} = i\left(\beta_s - \frac{1}{2}\omega_s \mathbf{B}\cdot\boldsymbol{\sigma}\right)|A_s\rangle + \frac{2i\gamma}{3}\left(\langle A_p|A_p\rangle + |A_p\rangle\langle A_p| + |A_p^*\rangle\langle A_p^*|\right)|A_s\rangle + \frac{i\gamma}{3}\left(\langle A_p^*|A_p\rangle + 2|A_p\rangle\langle A_p^*|\right)|A_i^*\rangle, \tag{2}$$

where ω_j and β_j ($j = p, s, i$) are the optical frequencies and the propagation constants, respectively, for the three waves, and γ is the nonlinear parameter.[4] The idler equation can be obtained by interchanging the subscripts s and i in Eq. (2). The three components of vector $\boldsymbol{\sigma}$ represent the Pauli matrices.[5]

Several approximations were made in deriving Eqs. (1) and (2). Fiber losses were neglected because of the short fiber lengths commonly used for making FOPAs. We also neglected pump depletion because the pump power is much larger than the signal and idler powers in practice. For the same reason, self-phase modulation is included for the pump but neglected for the signal and idler. Equation (2) includes cross-phase modulation (XPM) induced by the pump because XPM affects phase matching of the FWM process and leads to nonlinear polarization rotation of the signal and idler waves.

Vector $\mathbf{B}$ governs the birefringence-induced random SOP variations. Because the beat length and correlation length of residual birefringence are ~10 m for silica fibers,[9,10] both lengths are much shorter than the length scale over which nonlinear polarization rotation occurs (~1 km). Thus rapid SOP variations associated with the pump can be averaged; their main effect is to reduce the nonlinear parameter such that its effective value $\gamma_e = 8\gamma/9$ (Ref. 11) and results in a polarization-independent self-phase modulation. Next we note that what matters for XPM and FWM is the relative orientation of the pump and signal or idler SOPs. We thus choose to work in a rotating frame in which the pump SOP remains fixed. Making a further transformation as $|A\rangle = |A'\rangle\exp[i\int_0^z(\beta_p + \gamma_e P_0)\mathrm{d}z]$, where $P_0 = \langle A_p|A_p\rangle$ is the pump power, the signal and idler equations reduce to

$$\frac{\mathrm{d}|A_s\rangle}{\mathrm{d}z} = i\left(\Delta\beta_s - \frac{1}{2}\Delta\omega\,\mathbf{b}\cdot\boldsymbol{\sigma}\right)|A_s\rangle + i\gamma_e\left(\langle A_p|A_s\rangle + \langle A_i|A_p\rangle\right)|A_p\rangle, \tag{3}$$

$$\frac{\mathrm{d}|A_i\rangle}{\mathrm{d}z} = i\left(\Delta\beta_i + \frac{1}{2}\Delta\omega\,\mathbf{b}\cdot\boldsymbol{\sigma}\right)|A_i\rangle + i\gamma_e\left(\langle A_p|A_i\rangle + \langle A_s|A_p\rangle\right)|A_p\rangle, \tag{4}$$

where $\Delta\beta_j = \beta_j - \beta_p$ ($j = s, i$), $\Delta\omega = \omega_s - \omega_p$, and we have dropped the prime for simplicity. Vector $\mathbf{b}$ is

related to **B** by a rotation in the Stokes space and is responsible for PMD. Since the fiber length is typically much longer than the birefringence correlation length, we model **b** as a three-dimensional stochastic process such that $\overline{\mathbf{b}(z)} = 0$ and $\overline{\mathbf{b}(z_1)\mathbf{b}(z_2)} = (D_p^2/3)\vec{I}\delta(z_2 - z_1)$, where the overbar denotes an average over random birefringence changes, $\vec{I}$ is the second-order unit tensor, and D_p is the PMD parameter.

In the absence of birefringence, Eqs. (3) and (4) reduce to the scalar case when the three waves are linearly copolarized since they maintain their input SOP. In the presence of residual birefringence, the XPM and FWM processes depend only on $\langle A_s|A_p\rangle$ and $\langle A_i|A_p\rangle$. Since PMD changes the SOPs of the signal and idler with respect to the pump randomly along the fiber, the XPM and FWM efficiencies vary randomly in different sections of fiber. Consequently, the amplified signal and idler powers fluctuate from fiber to fiber even if the fibers are otherwise identical. For the same reason, these powers can fluctuate with time for a given FOPA at time scales associated with environmental variations.[2] The inset of Fig. 1 shows examples of such variations in the FOPA gain spectrum for $D_p = 0.05$ ps/km$^{1/2}$.

The general solution of Eqs. (3) and (4) requires a numerical approach. However, it turns out that the evolution of the signal and idler powers, $S_0 = \langle A_s|A_s\rangle$ and $I_0 = \langle A_i|A_i\rangle$, is determined by the relationship among the Stokes vectors of the three waves, $\mathbf{P} \equiv \langle A_p|\boldsymbol{\sigma}|A_p\rangle$, $\mathbf{S} \equiv \langle A_s|\boldsymbol{\sigma}|A_s\rangle$, $\mathbf{I} \equiv \langle A_i|\boldsymbol{\sigma}|A_i\rangle$, and the complex variables $\rho_j \equiv \langle A_j|A_p\rangle$ and $\Gamma_j \equiv \langle A_j|\boldsymbol{\sigma}|A_p\rangle$ ($j = s, i$), which are associated with the relative orientations between the pump and the signal or the idler SOPs. The average gain and signal-power fluctuations are obtained by use of $G_{\mathrm{av}} = \overline{S_0(L)}/S_0(0)$ and $\sigma_s^2 = \overline{S_0^2(L)}/\overline{S_0(L)}^2 - 1$.

Finding the evolution equations for S_0 and I_0 from Eqs. (3) and (4) and averaging them over the birefringence fluctuations by following the technique used in Ref. 12, we obtain the following equations governing the average signal and idler powers:

$$\frac{d\overline{S_0}}{dz} = \frac{d\overline{I_0}}{dz} = \gamma_e P_0 \Re(U), \tag{5}$$

$$\frac{dU}{dz} = -(\eta/2 + i\kappa)U + \gamma_e P_0(\overline{S_0} + \overline{I_0} + V), \tag{6}$$

$$\frac{dV}{dz} = -\eta V + 2\gamma_e P_0 \Re(U), \tag{7}$$

where $\Re$ denotes the real part, $\eta = 1/L_d = D_p^2(\Delta\omega)^2/3$, and L_d is the PMD diffusion length. The auxiliary variables U and V are defined as $U = 2i\overline{\rho_s\rho_i}/P_0$ and $V = (\overline{\mathbf{S}} + \overline{\mathbf{I}}) \cdot \hat{p}$, where $\hat{p} = \mathbf{P}/P_0$ is the unit vector along the pump SOP. Also, $\kappa = \beta_s + \beta_i - 2\beta_p + 2\gamma_e P_0$ describes the net phase mismatch among the three waves.

Equations (5)–(7) are easy to solve to obtain the average FOPA gain spectrum. Although such an average gain spectrum does not correspond to a single experimental measurement, it provides a good indication of the effect of PMD on FOPA performance. Figure 1 shows such gain spectra for two D_p values when the input signal is linearly copolarized with the pump. The solid curves show the analytical results with $\gamma = 2$ W^{-1}/km, $L = 2$ km, $\lambda_0 = 1550$ nm, $\beta_3 = 0.1$ ps^3/km, $\beta_4 = 1 \times 10^{-4}$ ps^4/km, and $P_0 = 1$ W. The dotted curve shows for comparison the case of an isotropic fiber without birefringence. The pump wavelength ($\lambda_p = 1550.15$ nm) was chosen such that the signal has a fairly flat gain over a 40-nm bandwidth in the absence of birefringence. Since the FOPA gain is susceptible to any perturbations to the phase-matching condition, PMD-induced random variations of the signal and idler SOPs affect the average gain spectra considerably. Their effect increases with increased wavelength separation between the pump and the signal. As a result, PMD not only reduces the peak gain value but also severely degrades the flatness of the gain spectrum.

When signal wavelength λ_s is close to the pump, the PMD diffusion length becomes longer than the FOPA length, and the signal and idler can remain nearly copolarized with the pump along the fiber. The effect of PMD is small in this region, and the FOPA gain is reduced by only 1 dB or so because of the reduction in γ by a factor of 8/9. When λ_s is relatively far from λ_p, the situation becomes different because the PMD diffusion length is now comparable with or even shorter than the FOPA length. As a result, PMD induces considerable random variations in the signal and idler SOPs, leading to further reduction in the FOPA gain and severe degradation of the gain uniformity. Even for a small D_p value of 0.05 ps/km$^{1/2}$ a significant tilt appears in the gain spectrum. For larger values of D_p the gain spectrum is degraded even more. For example, $L_d = 2.16$ km for $|\lambda_s - \lambda_p| = 30$ nm when $D_p = 0.05$ ps/km$^{1/2}$, but this value reduces to 0.24 km

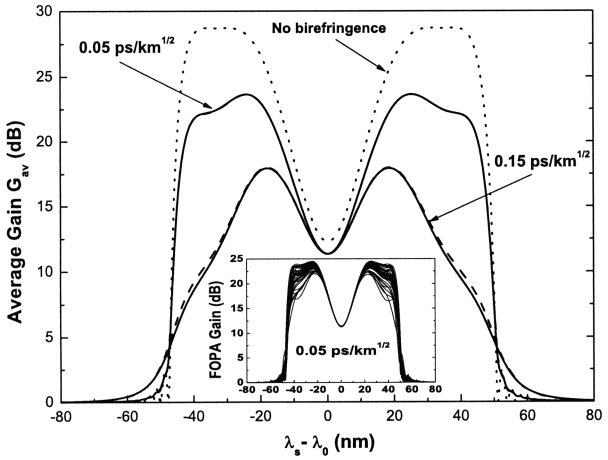

Fig. 1. Average FOPA gain as a function of signal detuning from the zero-dispersion wavelength for two values of D_p. Solid and dashed curves show the analytical and numerical results, respectively; two curves cannot be distinguished for $D_p = 0.05$ ps/km$^{1/2}$ on the scale used. The dotted curve shows for comparison the case without birefringence. The inset shows examples of FOPA gain spectra numerically obtained from Eqs. (1) and (2) for different realizations of residual birefringence.

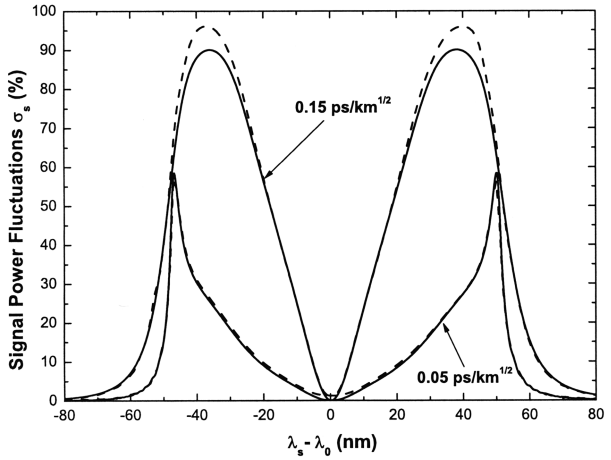

Fig. 2. Signal fluctuation level σ_s plotted as a function of signal detuning, under conditions of Fig. 1.

when $D_p = 0.15$ ps/km$^{1/2}$. As a result, the average gain spectrum is distorted drastically for such large values of D_p.

To justify the approximations made in deriving the averaged equations, we performed numerical simulations with the full vector model based on Eqs. (1) and (2) and dividing the fiber into many 10-m-long sections. Birefringence was kept constant inside each section but changed randomly from section to section. The signal and idler powers were averaged over 500 runs. The analytical results based on Eqs. (5)–(7) agree well with the simulation results (dashed curve).

PMD-induced signal fluctuations are quantified by the variance of the amplified signal. This quantity is related to the second-order moments and correlations of S_0, $\mathbf{S}$, I_0, $\mathbf{I}$, ρ_s, ρ_i, $\mathbf{\Gamma}_s$, and $\mathbf{\Gamma}_i$ and can be calculated by solving a set of coupled averaged equations (not reproduced here because of their lengthy nature). Figure 2 shows the level of signal fluctuations as a function of signal detuning for the same parameters used for Fig. 1. When λ_s is close to λ_p, fluctuations are small because the PMD diffusion length is much longer than the FOPA length. However, the level of fluctuations increases quickly in the useful region where gain is large. Over the main peak of the gain spectrum, output signal fluctuations can exceed 30% even for a relatively small value of $D_p = 0.05$ ps/km$^{1/2}$. Signal fluctuations increase drastically for $D_p = 0.15$ ps/km$^{1/2}$, approaching 90%. Numerical simulations (dashed curves) agree well with this analytical prediction.

Although Figs. 1 and 2 focus on signal amplification, the theory and the results also apply for wavelength converters because the idler power is related to the signal power as $I_0(L) = S_0(L) - S_0(0)$. Since the conversion efficiency ζ is related to the signal gain G as $\zeta \equiv I_0(L)/S_0(0) = G - 1$, the average conversion efficiency $\bar{\zeta} = G_{\rm av} - 1$. The level of idler-power fluctuations is related to that of the signal simply as $\sigma_i^2 \equiv \overline{I_0^2(L)}/\overline{I_0(L)}^2 - 1 = \sigma_s^2 G_{\rm av}^2/(G_{\rm av} - 1)^2$. The curves in Figs. 1 and 2 can be used to find $\bar{\zeta}$ and σ_i with the above relations. In particular, all the qualitative features of these figures apply to wavelength converters as well.

The preceding analysis is based on the assumption that the correlation length l_c of birefringence fluctuations is much shorter than the fiber length. One might ask whether this assumption is justified for fiber lengths <1 km. Extensive numerical simulations show that our analytic theory works well as long as the FOPA length exceeds $10-15 l_c$. The results shown in Figs. 1 and 2 change by only a small amount even when l_c is as long as 100 m for a 2-km-long FOPA. High-nonlinearity fibers are increasingly being used for making FOPAs, and lengths of ~100 m are sufficient for them. Our analytic results apply in this case for $l_c = 10$ m but become questionable when l_c exceeds 50 m. Residual birefringence can no longer be treated as white noise in this case and a numerical approach should be used.

In summary, we have developed a vector theory of the degenerate FWM process inside optical fibers and have used it to study the effect of PMD on the performance of FOPAs and wavelength converters. We found that PMD not only changes the average value of the gain significantly but also introduces considerable signal fluctuations. For typical values of D_p (around 0.05 ps/km$^{1/2}$), fluctuations are in the 20–30% range over the flat region of the gain spectrum. The bandwidth of the FOPA gain spectrum may be limited by other factors related to fiber dispersion, but PMD is also likely to be a major limiting factor for modern FOPAs. As a rough guide, the average differential group delay of the fiber $[D_p(8L/3\pi)^{1/2}]$ should be less than 50 fs to keep the PMD-induced signal fluctuations below 10% over the main portion of the gain spectrum.

We thank S. Radic for helpful discussions. This work was supported by the National Science Foundation under grants ECS-0320816 and ECS-0334982.

References

1. J. Hansryd, P. A. Andrekson, M. Westlund, J. Li, and P. O. Hedekvist, IEEE J. Sel. Top. Quantum Electron. **8,** 506 (2002).
2. M. N. Islam and Ö. Boyraz, IEEE J. Sel. Top. Quantum Electron. **8,** 527 (2002).
3. S. Radic, C. McKinstrie, and R. Jopson, Opt. Fiber Technol. Mater. Devices Syst. **9,** 7 (2003).
4. G. P. Agrawal, *Nonlinear Fiber Optics*, 3rd ed. (Academic, New York, 2001).
5. J. P. Gordon and H. Kogelnik, Proc. Natl. Acad. Sci. USA **97,** 4541 (2000).
6. K. Inoue, IEEE J. Quantum Electron. **28,** 883 (1992).
7. P. O. Hedekvist, M. Karlsson, and P. A. Andrekson, IEEE Photon. Technol. Lett. **8,** 776 (1996).
8. O. Aso, S. Arai, T. Yagi, M. Tadakuma, Y. Suzuki, and S. Namiki, IEICE Trans. Electron. **E83-C,** 816 (2000).
9. A. Galtarossa, L. Palmieri, M. Schiano, and T. Tambosso, Opt. Lett. **25,** 384 (2000).
10. A. Galtarossa, L. Palmieri, M. Schiano, and T. Tambosso, Opt. Lett. **26,** 962 (2001).
11. P. K. A. Wai and C. R. Menyuk, J. Lightwave Technol. **14,** 148 (1996).
12. Q. Lin and G. P. Agrawal, J. Opt. Soc. Am. B **20,** 1616 (2003).